Near-infrared fluorescence spectroscopy of single-walled carbon nanotubes and its applications

Hongduan Huang, Mingjian Zou, Xiao Xu, Xinyi Wang, Feng Liu, Na Li

Semiconducting single-walled carbon nanotubes (SWCNTs) emit fluorescence at near-infrared (NIR) wavelengths that are characteristic of the specific diameter and the chiral angle. While providing a convenient method for structural identification of semiconducting SWCNTs, NIR fluorescence of SWCNTs also offers a powerful approach for sensor development and *in vivo* or real-time imaging of biological systems.

This article provides an introductory overview of the approaches to obtaining individually dispersed semiconducting SWCNTs with reasonably good purity, which is a critical step in acquiring NIR fluorescence spectra. It also summarizes the progress since 2002 in sensor design and applications in bioimaging *in vitro* and *in vivo* using NIR fluorescence of semiconducting SWCNTs.

Keywords: Bioimaging; Biological system; Chiral angle; Near-infrared fluorescence spectroscopy; Real-time imaging; Sensor; Single-walled carbon nanotube; Specific diameter; Structural identification; SWCNT

Hongduan Huang, Mingjian Zou, Xiao Xu, Feng Liu, Na Li*
Beijing National Laboratory for Molecular Sciences (BNLMS), Key Laboratory of Bioorganic Chemistry and Molecular Engineering of the Ministry of Education, Institute of Analytical Chemistry, College of Chemistry and Molecular Engineering, Peking University, Beijing 100871, China

Xinyi Wang,
College of Sciences, Shenyang Agricultural University, Shenyang 110161, China

*Corresponding author.
Tel.: +86 10 62761187;
Fax: +86 10 62751708;
E-mail: lina@pku.edu.cn

1. Introduction

The carbon nanotube (CNT) is an allotrope of carbon-like graphite, diamond and fullerene. The unique structure and properties of CNTs have become widely recognized since Iijima's breakthrough studies using transmission electron microscopy in 1991 [1]. Defect-free CNTs are classified as single-walled CNTs (SWCNTs) and multi-walled CNTs (MWCNTs). The SWCNT can be visualized as a hollow, seamless cylinder rolled from a single-layer graphene sheet, while the MWCNT is a collection of concentric SWCNTs with different diameters. Every possible SWCNT structure can be uniquely characterized by a vector $\boldsymbol{C}$ ($\boldsymbol{C} = n\mathbf{a_1} + m\mathbf{a_2}$), with $\boldsymbol{a}_1$ and $\boldsymbol{a}_2$ as graphene lattice vectors (Fig. 1) [2]. The two integers (n,m) are commonly used to label the structures of SWCNTs, providing the information on the diameters and chiral angles of the CNTs. Structures for which the difference n-m is evenly divisible by 3 show metallic or semimetallic characteristics, whereas the others exhibit semiconducting characteristics.

Due to their size, shape, unique structure, and physical properties, CNTs have found applications in many fields, including field-effect transistors (FETs), biosensors and drug-delivery vehicles. Specifically, the remarkable one-dimensional quantum effect imparts distinctive optical properties to SWCNTs, which have strong optical absorption in the near-infrared (NIR) range called the therapeutic IR window (700–1100 nm, depending on body-tissue type), so they can be used for photothermal therapy and photoacoustic imaging [3]. With diameters of 1–2 nm, lengths ranging from as short as 50 nm up to 1 cm, and all atoms exposed on the surface, SWCNTs have ultrahigh surface area (theoretically 1300 m^2/g) [3]. Together with the strong absorbance in the NIR range, semiconducting SWCNTs are promising vehicles for targeted drug delivery and transducers for biosensing [4]. As mentioned above, SWCNTs have semiconducting or metallic properties

0165-9936/$ - see front matter © 2011 Elsevier Ltd. All rights reserved. doi:10.1016/j.trac.2011.03.014

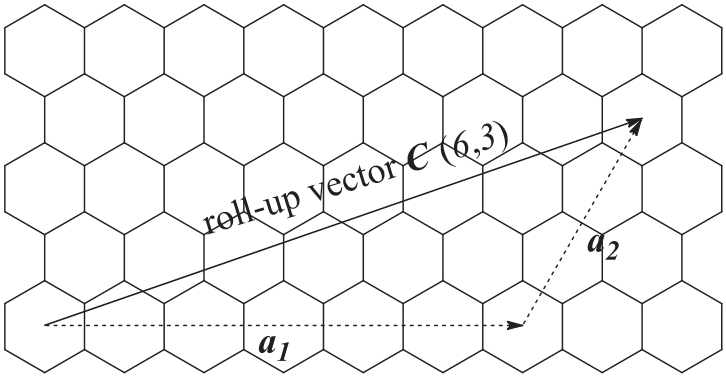

Figure 1. Roll-up vector $\boldsymbol{C}$ and graphene-lattice vectors $\boldsymbol{a}_1$ and $\boldsymbol{a}_2$. $\boldsymbol{C} = n\mathbf{a_1} + m\mathbf{a_2}$ (modified from [2]).

depending on their structures. Usually, semiconducting tubes can be used for metal-semiconductor (Schottky) diodes, pn-junction diodes, and FETs, whereas metal tubes are used for single-electron tunneling transistors [4].

SWCNTs offer a direct band gap and a well-defined band and sub-band structure, which make them ideal candidates for optics and optoelectronics. Much research has focused on resonance Raman spectroscopy, ultraviolet to NIR (UV-VIS-NIR) spectroscopy [4], and Rayleigh scattering spectroscopy of a single SWCNT [5]. The intrinsic NIR fluorescence is a recently discovered optical property of the individual semiconducting SWCNT [6]. Due to the high sensitivity, photostability, and negligible autofluorescent background at NIR wavelengths in biological media, the fluorescence of SWCNTs opens new avenues for highly effective detection in complex environmental and biological systems. This review will focus on the intrinsic fluorescence characteristics of SWCNTs and their applications in SWCNT structural characterization, biosensors, and optical imaging in live cells and tissues in the past few years since the fluorescence of SWCNTs was elucidated.

2. Fluorescence of SWCNTs

In 2002, the group led by Weisman and Smalley [6] separated and solubilized semiconducting SWCNTs in aqueous sodium dodecyl sulfate (SDS) surfactant by sonication, and for the first time observed the NIR fluorescence of SWCNTs, which can be explained by the density of states of the SWCNTs. Quasi-one-dimensionality of individual semiconducting SWCNT causes the density of electronic states to have a series of sharp peaks, named van Hove singularities (HVSs), with energies dependent mainly on tube diameter. The energy levels of an individual semiconducting SWCNT are illustrated in Fig. 2 [2]. The energy of the Fermi level is defined as zero, and energy levels above and below the Fermi level are conduction and valence bands, respectively. The optical transition occurs when an electron or a hole is excited from one energy level to another, denoted E_{pq}, with p and q representing the order of conduction and valence bands, respectively. Transition is allowed only when $p = q$ (e.g., E_{11}, E_{22}, and E_{33}).

The emission and absorption spectra in the first van Hove transition (E_{11}) of the same sample are strikingly correspondent [6], so the fluorescence can be assigned to the E_{11} emission of semiconducting SWCNTs. It is proposed that the excitation of the semiconducting SWCNT in the second van Hove transition, E_{22}, is followed by fast electronic relaxation before fluorescence emission in the first van Hove transition, E_{11} (Fig. 2).

3. Obtaining fluorescent SWCNTs

The low fluorescence quantum yields (10^{-4}–10^{-2}) have been a challenge in the field of SWCNT optics [7]. The quantum yield of ensembles that included defective SWCNTs and residual bundles was estimated to be 0.1% [2]. Further study found that the intrinsic SWCNT quantum yield is much higher than previously reported. With better sample preparation and experimental conditions, the quantum yield was determined to approach 10% [8,9]. The quantum yield of fluorescence is therefore closely associated with the quality of SWCNTs and the dispersion efficiency [10]. High-quality SWCNTs are samples that are to a large extent free from undesired species, including MWCNTs, metallic, aggregated or damaged SWCNTs, amorphous carbon, residual catalysts, giant fullerenes, and other impurities. All the above-mentioned species absorb light like SWCNTs, but only the individually dispersed and undamaged semiconducting SWCNTs emit fluorescence in the NIR region.

Synthetic methods determine the quality of CNTs [11]. Arc discharge, laser ablation and chemical-vapor deposition (CVD) are the methods generally used to produce

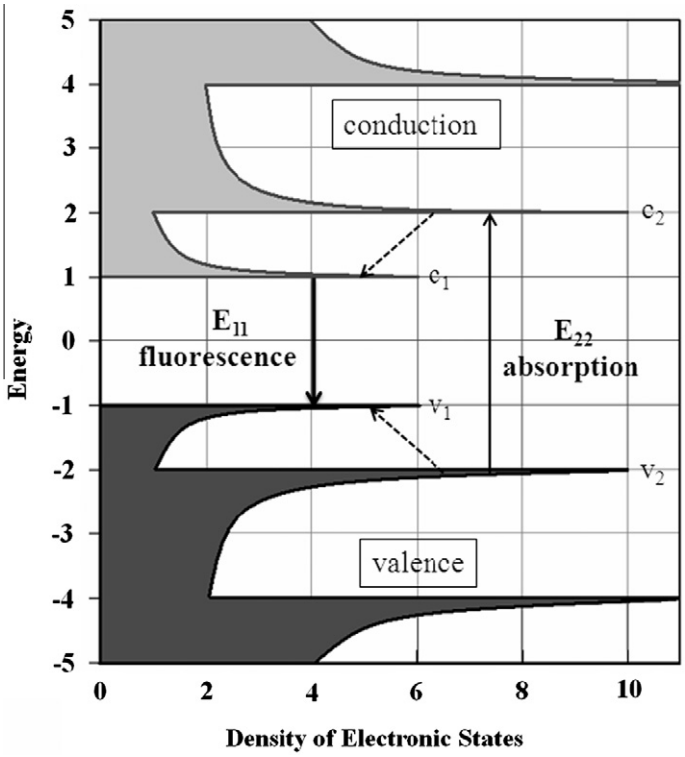

Figure 2. Density of electronic states for a single semiconducting nanotube structure (modified from [2]).

CNTs. Generally speaking, laser ablation produces clean CNTs with relatively low yield, whereas arc discharge produces large quantities of material with poor purity. Compared with arc discharge and laser ablation, CVD is a low-temperature method to produce CNTs, and is very easy to scale up. However, traditional CVD processes yield MWCNTs or poor quality SWCNTs with a large diameter distribution. Because of the uncertainty of purity and/or poor feasibility for scale-up production, more advanced synthetic methods are most desirable. The CoMoCat process [12] and the high-pressure CO disproportionation process (HiPco) [13] were specifically developed for CVD synthesis, and can produce SWCNTs of relatively high quality.

The approaches to purification of SWCNTs include structure-selective and size-selective separations. The former is to remove the structural impurities generated in the synthesis steps, and the latter produces a homogeneous diameter or size distribution. The commonly used purifying techniques are oxidation [14], acid treatment [14], annealing [14], ferromagnetic separation [15], ultrasonication [16], microfiltration [17], cutting [18], functionalization [19], ultracentrifugation [20–23] and chromatographic separation [24]. Carbonaceous impurities can be removed by oxidation, but SWCNTs may also be oxidized. Metallic catalysts can be eliminated with acid treatment. HNO_3 is generally preferred over HCl, because HCl may affect the SWCNTs and other carbon particles. Magnetic particles can be removed by ferromagnetic separation. SWCNTs with narrow distribution of length and diameter can be obtained with chromatographic separation and ultracentrifugation.

The preparative ultracentrifuge has proved to be an essential tool for processing CNTs. In particular, density-gradient ultracentrifugation (DGU) was first introduced by Arnold and co-workers [20,21] and recently emerged as a technique for sorting SWCNT mixtures into their distinct (*n*,*m*) structural forms. Arnold and co-workers [21] isolated narrow distributions of SWCNTs in which >97% were within a 0.02-nm diameter distribution using structure-discriminating surfactants to introduce subtle differences in their buoyant densities. Bulk quantities of SWCNTs containing predominantly a single electronic type were also produced in the same laboratory with the aid of competing mixtures of surfactants.

The work of Arnold et al. [23] on the hydrodynamic properties of surfactant-encapsulated SWCNTs by optically measuring their spatial and temporal redistribution in situ in an analytical ultracentrifuge provides a guide for designing centrifuge-based processing procedures for preparing samples of SWCNTs for specific applications.

Ghosh et al. [25] used tailored non-linear density gradients to expand the separation capacity of DGU. In

their work, highly polydisperse samples of SWCNTs grown by the HiPco method were sorted in a single step to give fractions enriched in any of 10 different (*n*,*m*) species. In addition, armchair and near-armchair species can also be enriched from as-prepared CNT samples using modified DGU [26]. Generally, one or more of the above-mentioned purification processes are necessary to obtain the SWCNTs with pronounced fluorescence spectra. In addition, the process variables (e.g., temperature and duration) should be carefully controlled.

Other than the quality of SWCNTs, a well-dispersed SWCNT suspension is another requirement to obtain a good fluorescence spectrum [3]. Substantial success has been attained in obtaining such SWCNT suspensions. The dispersing methods mainly include both chemical functionalization [27] of SWCNT surfaces and physical dissolution by breaking the π–π interactions of SWCNTs with the aid of surfactants [6], biomolecules (nucleic acids, phospholipids, and proteins) [28–31], organic solvents [32], polymers [33,34], and silica [35]. Chemical functionalization usually causes damage to the original structure of SWCNTs, resulting in fluorescence quenching, so physical dissolution is more favored. Surfactants {e.g., SDS [2,6,36,37], sodium cholate [29,38] and sodium dodecyl benzene sulfonate (SDBS) [36,39]} are most frequently used to solubilize SWCNTs. Biomolecules, namely nucleic acids [29,40,41], phospholipids [42] and proteins [28], have attracted much attention in the separation of SWCNTs, because of the potential applications in biochemical and medical fields. Dai and co-workers [30,43,44] used PEGlated phospholipids (PEG-polyethyleneglycol) to solubilize and to functionalize SWCNTs. PEGlated phospholipids are biocompatible and non-toxic. This type of biomolecule can also preserve the intrinsic fluorescence of SWCNTs, while providing functional groups for bioconjugation with antibodies or other molecules [3]. Since there are strong π-π interactions between SWCNT walls, intense and prolonged sonication is compulsory. After sonication, tube bundles and residual catalyst particles precipitate with centrifugation. The individually dispersed SWCNTs obtained in this manner emit distinctive NIR fluorescence when excited by red light (usually 500–900 nm, with excitation at 532 nm, 658 nm, and 785 nm frequently used).

4. Applications of NIR fluorescence of SWCNTs

In the past decade, semiconducting SWCNT band-gap fluorescence in the NIR region has been a new focus of this extraordinary material. In addition to high-resolution transmission electron microscopy, scanning probe microscopy, and absorption spectroscopy in UV, Vis, and NIR regions, intrinsic fluorescence provides a new approach for SWCNT structural characterization. With larger Stokes shifts compared to traditional organic fluorophores, SWCNTs are advantageous for convenient optical filtering and efficient detection. The photostability at high excitation power and the short excited-state lifetime of SWCNTs allow many rapid cycles of excitation and emission for a single illuminated SWCNT, which results in a bright optical signal although the emissive quantum yield is less than a few percent [10]. Because the detection is made in the NIR region, autofluorescence from the sample background (usually 300–800 nm, depending on the fluorescent molecules in the sample) is negligible. All the above features make the SWCNT a promising fluorescent probe for sensor development as well as *in vitro* and *in vivo* imaging of biological systems.

4.1. Structure identification for SWCNTs

To know the identity and relative abundances of (*n*,*m*) species in an SWCNT sample is very important because the electronic, optical, chemical, and mechanical properties of SWCNTs depend on their structure. The current single-particle microscopic methods that can be used to identify the specific (*n*,*m*) structure and determine the abundances (e.g., high-resolution scanning tunneling microscopy and electron nano-diffraction) require expensive instruments, well-trained personnel, and substantial measurement time, so they are impractical for routine analysis of bulk samples. NIR fluorescence provides a sensitive bulk method for assessing (*n*,*m*) contents. Smalley and Weisman's group [2] mapped every optical transition of interest in the fluorescence spectra (white oval in Fig. 3A) to specific (*n*,*m*) CNT structure (Fig. 3B). This work provided the detailed composition of a complex SWCNT sample, including information about the diameters and the chiral angles of the tubes. Weisman provided an insightful review on the capabilities, the limitations, and the future prospects for fluorimetric analysis in detailed structural characterization of bulk-SWCNT samples [10].

4.2. Optical sensors

In addition to characterizing the specific structure of SWCNTs, the NIR fluorescence of SWCNTs has also been used for development of optical sensors, generally with measurements based on the spectral shift or the fluorescence-intensity change when the analyte of interest is introduced.

The spectral shift is related to the change in the local dielectric environment surrounding SWCNTs created by solvents and adsorbed molecules, described as solvatochromism [45,46]. The observed energy shift, ΔE, can be explained as the change in the exciton-binding energy (E/eV), while E is inversely dependent on the squared value of local dielectric constant surrounding SWCNTs [29]. The local dielectric constant surrounding the

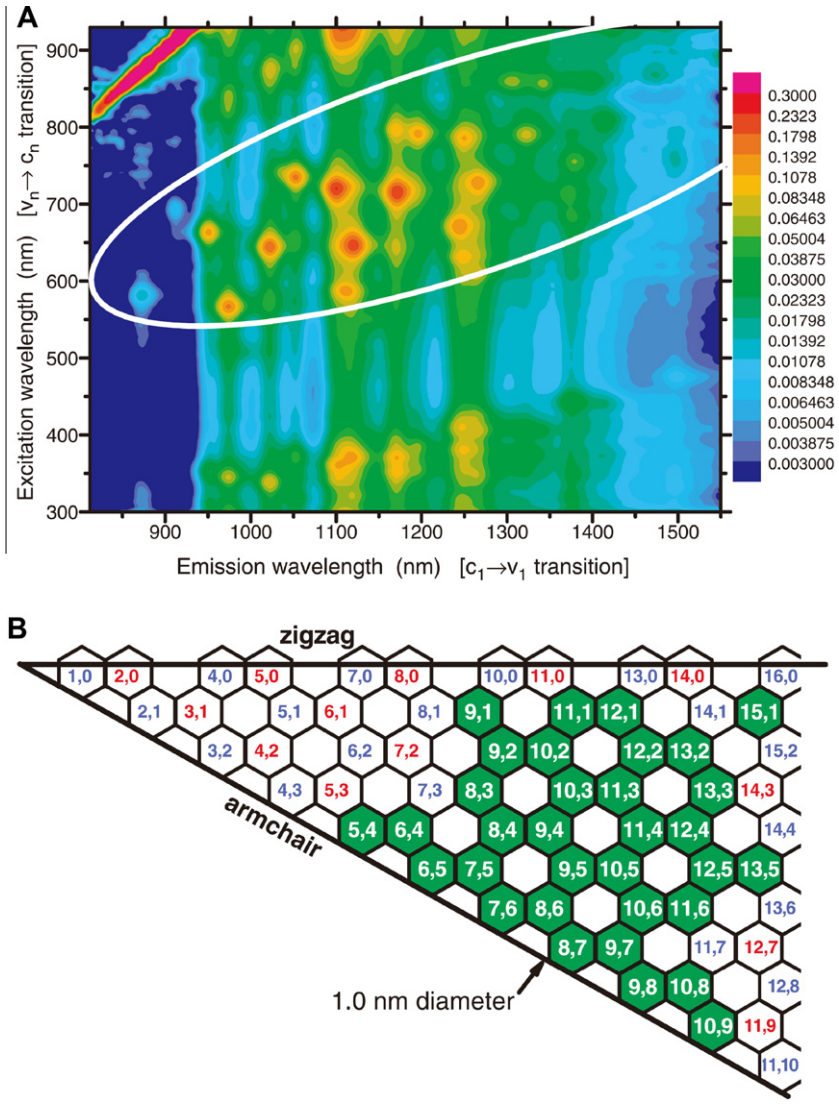

Figure 3. (A) Contour plot of fluorescence intensity *versus* excitation and emission wavelengths; and, (B) observed nanotube structures marked as green hexagons with white (*n,m*) labels on a graphene lattice (printed with permission from [2]).

SWCNTs is altered by the surface coverage of the SWCNTs. Thus, ΔE could be correlated to the fraction of unexposed SWCNT surface area, as described by a simplified variational model [29].

Choi et al. [45] developed a scaling model (revised Kataura plot) for predicting solvatochromic shifts of SWCNTs in various dielectric environments. In this work, the authors provided a detailed and insightful physics description of the model, and readers interested in solvatochromic shifting are referred to related publications [29,45–52].

The analyte inducing the change in the local dielectric constant surrounding the SWCNTs and thus altering the fluorescence spectrum of SWCNTs can be detected based on the spectral shift. Jeng [29] and co-workers detected DNA hybridization with modulation of the SWCNT band-gap fluorescence. The SWCNTs were first individually dispersed in 2% (wt) sodium-cholate aqueous solution. DNA was then assembled on the surface of SWCNTs by exchanging with the cholate in the suspension through dialysis, and the DNA-stabilized SWCNTs remained individually dispersed. Compared with cholate-stabilized SWCNTs, a red shift of 17.6 meV (15.6 nm) in emission peak was observed for DNA-assembled SWCNTs. Upon the addition of complementary DNA, a measurable energy increase of fluorescence emission was detected with a calculated limit of detection (LOD) of 6 nM, and the non-complementary DNA brought no significant change in the fluorescence emission.

By analyzing the blue shift in the NIR fluorescence, Jeng and co-workers [53] studied kinetics and

thermodynamics in hybridization. The results indicated that hybridization of DNA adsorbed to SWCNTs has much slower kinetics ($t_{1/2}$ = 3.4 h) than that of free solution DNA ($t_{1/2}$ = 4 min). Thermodynamics results showed that adsorption of the receptor-DNA strand to the CNT surface is consistent with models of polyelectrolyte adsorption on a charged surface, introducing both entropic (46.8 cal/mol/K) and activation energy (20.4 kcal/mol) barriers to the hybridization, which are greater than free solution values (31.9 cal/mol/K for entropy and 12.9 kcal/mol for activation energy) at 25°C. The authors also studied single-nucleotide polymorphism using the same method [38]. By analyzing the degree of blue shift of the emission spectra during the hybridization, complementary DNA and single-nucleotide polymorphism were distinguished.

Heller et al. [51] and Jin et al. [46] discovered that DNA immobilized on the surface of SWCNTs underwent conformational change when the specific interaction between DNA and divalent cations occurred. Such conformational change resulted in the change of the dielectric constant around the CNTs, so spectral shift would be expected. Also, the energy change is associated with the amount of the divalent ion added to the SWCNT suspension, with ion sensitivity in the order $Mg^{2+} < Ca^{2+} < Co^{2+} < Cu^{2+} < Hg^{2+}$. Since the NIR fluorescence of SWCNTs can operate in strongly scattering and absorbing media, the detection of DNA conformational polymorphism and divalent ions in whole blood, tissue and living cells is possible.

Some semiconducting SWCNT optical sensors have been developed based on the fluorescence-intensity change. One design uses electron-withdrawing agents to quench the fluorescence of SWCNTs. Introduction of the analyte consumes the electron-withdrawing agents, and the recovered fluorescence intensity is associated with the concentration of the analyte. In Barone's work [50], $Fe(CN)_6^{3-}$, the electron-withdrawing agent, was used for non-covalent functionalization of SWCNTs, so an optical glucose sensor was developed [50,54–56]. The surface of individually dispersed SWCNTs was first immobilized with glucose oxidase (GOx) by exchanging GOx with the stabilizing agent (cholate) via dialysis. The adsorption of $Fe(CN)_6^{3-}$ caused a decrease in the NIR fluorescence intensity. The quenched fluorescent emission was restored with addition of glucose, because the quenching agent, $Fe(CN)_6^{3-}$, was consumed by H_2O_2, which was the glucose-oxidation product catalyzed by GOx. The dynamic range of the method covered the general range of blood-glucose regulation in diabetic patients (1–8 mM), and had an LOD of 34.7 μM. Because of the advantages of the long-term photostability and fluorescence in the NIR region, which is preferred for *in vivo* detection, such enzyme-functionalized SWCNTs have the potential for implantation into thick tissue and whole-blood medium. Also, the design using electron-withdrawing molecules to modulate SWCNT fluorescence opened new ways for sensing, with choice of many other enzymes and electron-withdrawing molecules.

Dye-biotin conjugate-functionalized SWCNTs were used to monitor protein-binding events [57]. The dye (anthracene or phenylazoaniline) served as the oxidizing reagent to quench the NIR fluorescence of SWCNTs. When the interaction of biotin with avidin occurred, the fluorescence recovered with an LOD of 1 nM for avidin.

Jin et al. [58] developed an H_2O_2 optical sensor based on direct quenching of the NIR fluorescence of SWCNTs by H_2O_2. The authors demonstrated selective and single-molecule detection of H_2O_2, and imaged in real time with spatial precision the signaling flux emanating from single, living A431 human epidermal carcinoma cells. Quenchers {e.g., $Fe(CN)_6^{3-}$ and hydronium ion (H^+) [59] and others with oxidizing ability} can also be detected based on the quenching effect; however, the sensitivity depends greatly on the oxidizing ability of quenchers [54]. By analyzing the stochastic quenching of excitons as the quenchers adsorb to the SWCNT surface, the LOD was extended down to the single-molecule level.

Kim et al. [60] reported a nitric-oxide (NO) optical sensor using 3,4-diaminophenyl-functionalized dextran to disperse SWCNTs. In this design, the amines served as the electron-donating groups to confer more electron density and mobility on SWCNTs. Upon the addition of NO, the fluorescence was quenched due to electron transfer from the SWCNT to NO. The introduction of reducing agent (β-nicotinamide adenine dinucleotide, NADH) or removal of NO with dialysis resulted in complete recovery of fluorescence, and an LOD of 70 nM was achieved. Although the LOD was 12 times larger than the metal-fluorescein probe (5 nM), which involved the irreversible reduction of the metal (Cu^{II} to Cu^{I}) [61], this SWCNT-based probe could be used for the reversible detection of NO, enabling the regeneration of probes. Meanwhile, the good selectivity arising from the functional reagent (3,4-diaminophenyl-functionalized dextran), the resistance to photobleaching and the ability to penetrate deep into tissues allowed fast, selective *in vitro* and *in vivo* detection of nitric oxide.

The same group also successfully detected cellular ATP (adenosine 5′-triphosphate) using a luciferase-SWCNT conjugate [62], which is another design to induce fluorescence-intensity change. In this design, the fluorescence of SWCNTs was quenched by oxyLrin, the redox-quenching intermediate produced with the Luciferase-catalyzed bioluminescent reaction that involves selective consumption of ATP, the analyte (Fig. 4). By analyzing the intensity decrease of the NIR fluorescence, the amount of ATP was measured with an LOD of 240 nM. This sensor showed high selectivity towards ATP, but not the potential interfering molecules in cells, including AMP (adenosine 5′-monophosphate), ADP

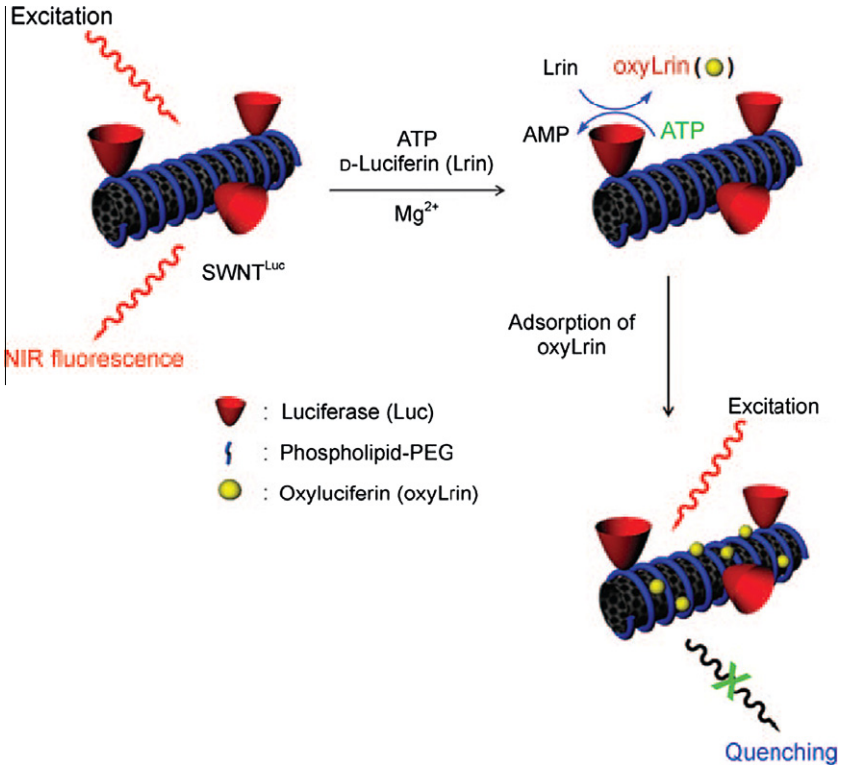

Figure 4. Optical sensor for ATP detection using the luciferase-SWCNT conjugate (printed with permission from [62]).

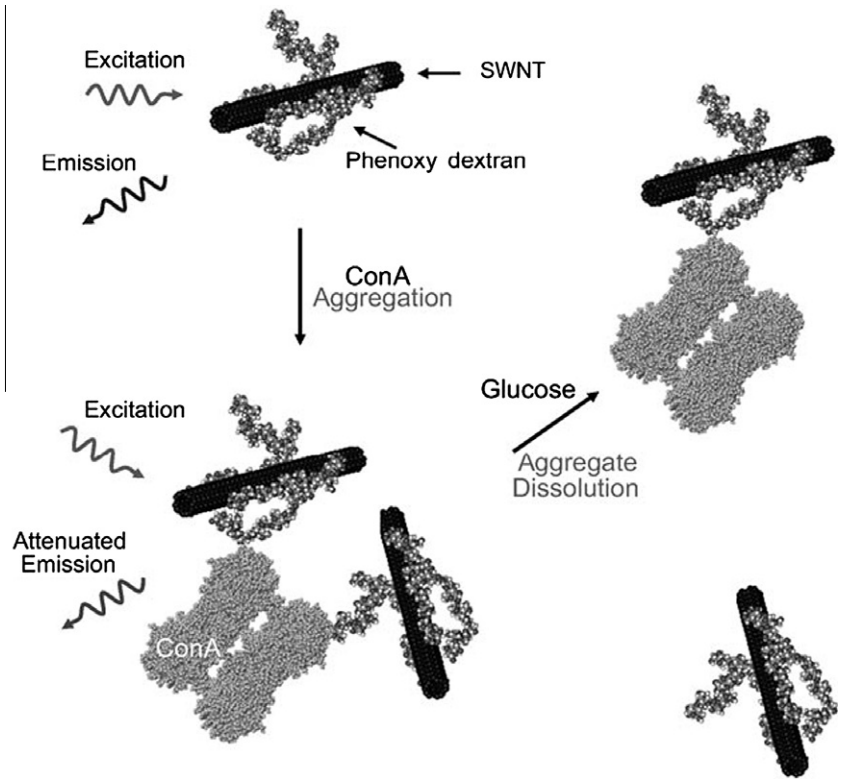

Figure 5. Operation of SWCNT affinity sensor (printed with permission from [52]).

(adenosine 5′-diphosphate), CTP (cytidine 5′-triphosphate) and GTP (guanosine 5′-triphosphate), indicating the possible application for cellular ATP detection. Moreover, the design based on generating the fluorescence quencher during the recognition of the target molecules could be applied to many other analytes.

Strano's group also demonstrated the detection of chemotherapeutic drugs and reactive oxygen species (ROSs), including alkylating agents (mechlorethamine, melphalan, and cisplatin), H_2O_2, $^{\bullet}OH$, and $^1O_2$, which involved both the emission-band intensity and wavelength changes [63]. The SWCNTs provide at least four modes that can be modulated to uniquely fingerprint species by the degree to which they alter the emission-band intensity and/or wavelength. Chemotherapeutic drugs and ROSs are important species in biological and life-science fields, but their short lifetime makes real-time or *in vivo* detection in live mammalian cells difficult. By using fluorescent SWCNTs, H_2O_2 was detected with single-molecule sensitivity. This work suggested significant and numerous diagnostic and metrological applications using semiconducting fluorescent SWCNTs to develop optical sensors.

Barone et al. [52,64] developed a glucose sensor using protein competitive binding assay. SWCNTs were first dispersed with phenoxy dextran. The phenoxy group was employed to increase the stability of SWCNT suspension, while the dextran functioned as an analogue and competitor of glucose to bind with Concanavalin A (ConA), a plant lectin with four saccharide-binding sites. When ConA was added to the suspension, aggregation of the dextran-CNT complex was produced and the fluorescence decreased due to the interaction of dextran with ConA. Once glucose was introduced, the aggregate was redispersed and the fluorescence increased because of the competitive binding of glucose with ConA (Fig. 5). In this case, glucose concentrations of 2–30 mM were measured with an LOD comparable to commercially available glucose sensors. Compared with the glucose sensors employing electron-withdrawing agents, which had a limited lifetime due to the consumption of the reagent

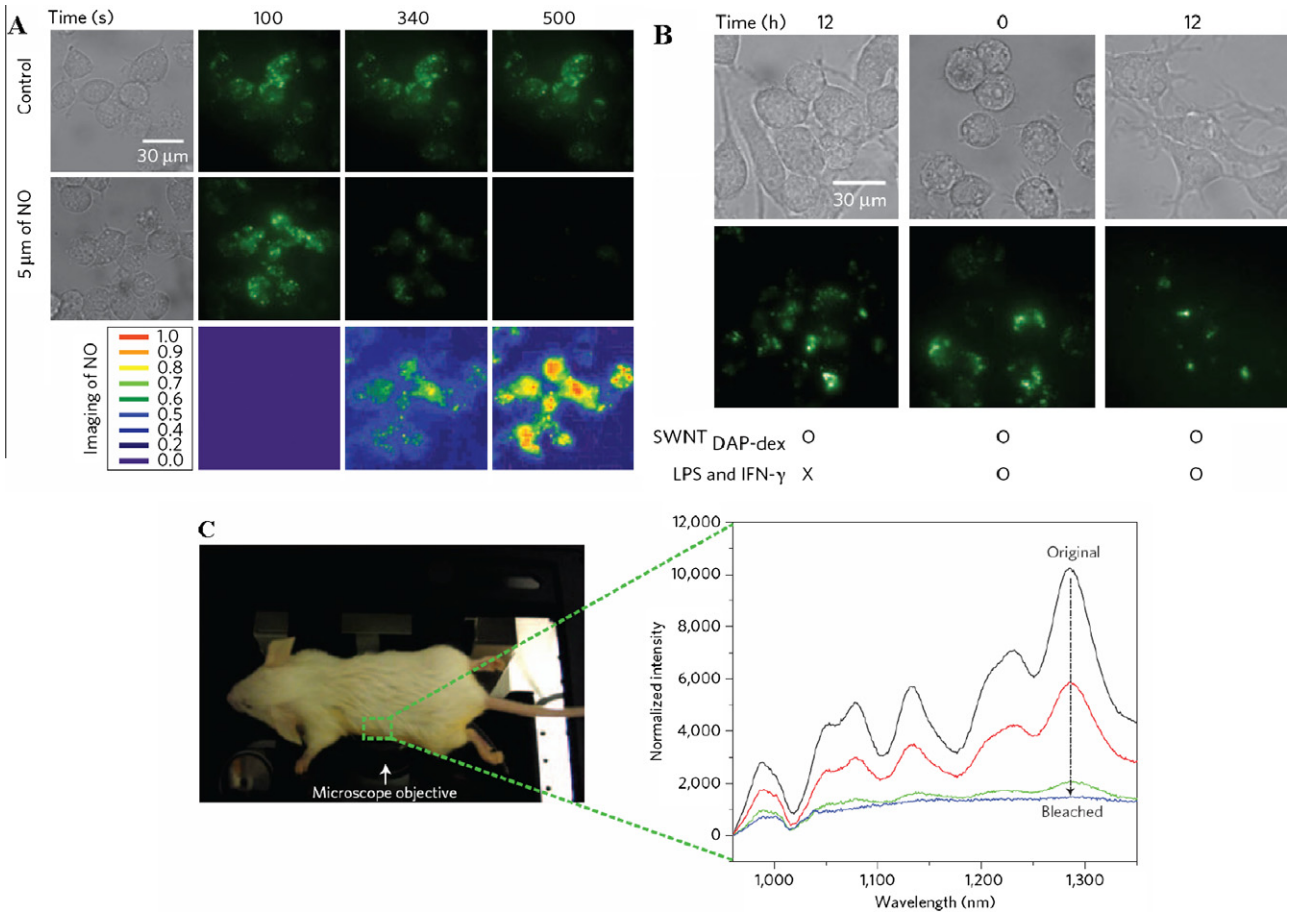

Figure 6. (A) NIR fluorescence images of Raw 264.7 murine macrophage cells incorporating SWCNTs before and after the addition of NO; (B) NIR fluorescence response to NO produced by iNOS in Raw 264.7 murine macrophage cells; and, (C) the potential of *in vivo* detection of NO and the NIR-fluorescence response to NO (60 μM) in the mouse (printed with permission from [60]).

($Fe(CN)_6^{3-}$), the sensors operating in a competitive manner had a longer lifetime favoring practical applications. Also, this glucose sensor could readily be implanted beneath the skin, producing a better detection output of fluorescence signals outside the skin and photostability compared with common organic and nanoparticle fluorophores.

4.3. NIR imaging in living tissues and cells

The optical properties of SWCNTs have unique advantages for biological samples. SWCNTs emit fluorescence in the NIR region, where most tissues exhibit greatly attenuated absorption, scattering and autofluorescence. The signal-to-noise ratio could therefore be significantly improved using SWCNTs as optical probes [65–67]. When combined with a fluorescence microscopic technique, SWCNT imaging provides a very useful tool for monitoring nucleic acids [68,69], proteins [70], and drugs [3] by mapping the location and the morphology of SWCNTs taken up by live tissues [71–73].

Cherukuri et al. [74] conducted the first work in microscopic imaging of SWCNTs in biological systems. They illustrated the ingestion of SWCNTs by mouse peritoneal macrophage-like cells using a spectrofluorimeter and a fluorescence microscope, suggesting future applications of SWCNTs in cell-biology research and medical diagnosis. Welsher et al. [75] successfully performed sensitive and selective live-cell detection using NIR-fluorescent SWCNTs. The polyethyleneglycol-functionalized SWCNTs were conjugated to antibodies to recognize receptors on cell surfaces (i.e. Rituxan for CD20 positive B-cells and Herceptin for HER2/neu positive breast cancer cells). The NIR fluorescence of SWCNTs provided a promising tool for probing specific binding of biological systems, as well as sensitive molecular detection and imaging at the cellular level.

Jin et al. [76,77] studied how SWCNTs were incorporated into and expelled from NIH-3T3 cells using real-time fluorescence measurement. The uptake process was found to depend on the length of SWCNTs [78]. SWCNTs longer than the length threshold (189 ± 17 nm) could not be taken up by the cells, so longer SWCNTs might be less toxic to cells than shorter ones. Heller and coworkers [79] found that SWCNT fluorescence remained stable in live cells for up to one week even under prolonged excitation. The mode of the wavelength-shift measurement could be applied to fabrication of long-term *in vitro* and *in vivo* optical sensors.

Substances that may exist in cells {e.g., glucose [50], NO [60], H_2O_2 [58], and ATP [62]} have also been detected. Kim et al. [60] achieved successful detection of NO in Raw 264.7 murine macrophage cells. Bleaching of the fluorescence of SWCNTs incubated in the cells could be clearly seen in the NIR-fluorescence images (Fig. 6A) after the cells were treated with NO. An LOD of 200 nM was reported. The spatial distribution of NO produced by iNOS (inducible NO synthase) in macrophage cells was also illustrated by fluorescent SWCNT imaging (Fig. 6B). Furthermore, the *in vivo* detection of NO was demonstrated by monitoring the fluorescence intensity in real time (Fig. 6C), and quenching was observed with the injection of NO.

5. Conclusion

As a new type of NIR fluorophore, SWCNTs have many advantages over the traditional organic fluorophores (e.g., good photostability, absence of photobleaching and freedom from interfering background emission in biological systems). Based on current progress, there will be more NIR-fluorescent SWCNT-sensor designs based on the measurement of the spectra, intensity, lifetime, and other fluorescent characteristics, and sensors with a combination of these characteristics. Also, one can expect continuous, long-term monitoring of life processes using band-gap fluorescence of uniquely functionalized SWCNTs. As more cost-effective approaches to producing large quantities of high-quality semiconducting SWCNTs become available, the NIR fluorescence of SWCNTs will find more applications in sensor development and bioimaging.

Acknowledgments

This work was supported by the National Natural Science Foundation of China (20975004). The authors thank John Hefferren for English editing.

References

[1] S. Iijima, Nature (London) 354 (1991) 56.
[2] S.M. Bachilo, M.S. Strano, C. Kittrell, R.H. Hauge, R.E. Smalley, R.B. Weisman, Science (Washington, DC) 298 (2002) 2361.
[3] Z. Liu, S. Tabakman, K. Welsher, H.J. Dai, Nano Res. 2 (2009) 85.
[4] M. Meyyappan, Carbon Nanotubes: Science and Application, CRC Press, Boca Raton, FL, USA, 2005.
[5] M.Y. Sfeir, F. Wang, L.M. Huang, C.C. Chuang, J. Hone, S.P. O'Brien, T.F. Heinz, L.E. Brus, Science (Washington, DC) 306 (2004) 1540.
[6] M.J. O'Connell, S.M. Bachilo, C.B. Huffman, V.C. Moore, M.S. Strano, E.H. Haroz, K.L. Rialon, P.J. Boul, W.H. Noon, C. Kittrell, J.P. Ma, R.H. Hauge, R.B. Weisman, R.E. Smalley, Science (Washington, DC) 297 (2002) 593.
[7] T. Hertel, S. Himmelein, T. Ackermann, D. Stich, J. Crochet, ACS Nano 4 (2010) 7161.
[8] D.A. Tsyboulski, J.D.R. Rocha, S.M. Bachilo, L. Cognet, R.B. Weisman, Nano Lett. 7 (2007) 3080.
[9] L.J. Carlson, S.E. Maccagnano, M. Zheng, J. Silcox, T.D. Krauss, Nano Lett. 7 (2007) 3698.
[10] R.B. Weisman, Anal. Bioanal. Chem. 396 (2010) 1015.
[11] E. Joselevich, H.J. Dai, J. Liu, K. Hata, A.H. Windle, Top. Appl. Phys. 111 (2008) 101.
[12] B. Kitiyanan, W.E. Alvarez, J.H. Harwell, D.E. Resasco, Chem. Phys. Lett. 317 (2000) 497.

[13] P. Nikolaev, M.J. Bronikowski, R.K. Bradley, F. Rohmund, D.T. Colbert, K.A. Smith, R.E. Smalley, Chem. Phys. Lett. 313 (1999) 91.
[14] Y.Q. Xu, H.Q. Peng, R.H. Hauge, R.E. Smalley, Nano Lett. 5 (2005) 163.
[15] L. Thien-Nga, K. Hernadi, E. Ljubovic, S. Garaj, L. Forro, Nano Lett. 2 (2002) 1349.
[16] P.X. Hou, C. Liu, Y. Tong, S.T. Xu, M. Liu, H.M. Cheng, J. Mater. Res. 16 (2001) 2526.
[17] K.B. Shelimov, R.O. Esenaliev, A.G. Rinzler, C.B. Huffman, R.E. Smalley, Chem. Phys. Lett. 282 (1998) 429.
[18] Z. Gu, H. Peng, R.H. Hauge, R.E. Smalley, J.L. Margrave, Nano Lett. 2 (2002) 1009.
[19] V. Georgakilas, D. Voulgaris, E. Vazquez, M. Prato, D.M. Guldi, A. Kukovecz, H. Kuzmany, J. Am. Chem. Soc. 124 (2002) 14318.
[20] M.S. Arnold, S.I. Stupp, M.C. Hersam, Nano Lett. 5 (2005) 713.
[21] M.S. Arnold, A.A. Green, J.F. Hulvat, S.I. Stupp, M.C. Hersam, Nat. Nanotechnol. 1 (2006) 60.
[22] F. Hennrich, K. Arnold, S. Lebedkin, A. Quintilla, W. Wenzel, M.M. Kappes, Phys. Status Solidi B 244 (2007) 3896.
[23] M.S. Arnold, J. Suntivich, S.I. Stupp, M.C. Hersam, ACS Nano 2 (2008) 2291.
[24] S. Niyogi, H. Hu, M.A. Hamon, P. Bhowmik, B. Zhao, S.M. Rozenzhak, J. Chen, M.E. Itkis, M.S. Meier, R.C. Haddon, J. Am. Chem. Soc. 123 (2001) 733.
[25] S. Ghosh, S.M. Bachilo, R.B. Weisman, Nat. Nanotechnol. 5 (2010) 443.
[26] E.H. Haroz, W.D. Rice, B.Y. Lu, S. Ghosh, R.H. Hauge, R.B. Weisman, S.K. Doorn, J. Kono, ACS Nano 4 (2010) 1955.
[27] J. Chen, M.A. Hamon, H. Hu, Y.S. Chen, A.M. Rao, P.C. Eklund, R.C. Haddon, Science (Washington, DC) 282 (1998) 95.
[28] R.J. Chen, Y.G. Zhang, D.W. Wang, H.J. Dai, J. Am. Chem. Soc. 123 (2001) 3838.
[29] E.S. Jeng, A.E. Moll, A.C. Roy, J.B. Gastala, M.S. Strano, Nano Lett. 6 (2006) 371.
[30] Z. Liu, W.B. Cai, L.N. He, N. Nakayama, K. Chen, X.M. Sun, X.Y. Chen, H.J. Dai, Nat. Nanotechnol. 2 (2007) 47.
[31] D.A. Tsyboulski, E.L. Bakota, L.S. Witus, J.D.R. Rocha, J.D. Hartgerink, R.B. Weisman, J. Am. Chem. Soc. 130 (2008) 17134.
[32] C.A. Furtado, U.J. Kim, H.R. Gutierrez, L. Pan, E.C. Dickey, P.C. Eklund, J. Am. Chem. Soc. 126 (2004) 6095.
[33] J. Chen, H.Y. Liu, W.A. Weimer, M.D. Halls, D.H. Waldeck, G.C. Walker, J. Am. Chem. Soc. 124 (2002) 9034.
[34] M.S. Strano, Nat. Mater. 5 (2006) 433.
[35] B.C. Satishkumar, S.K. Doorn, G.A. Baker, A.M. Dattellbaum, ACS Nano 2 (2008) 2283.
[36] V.C. Moore, M.S. Strano, E.H. Haroz, R.H. Hauge, R.E. Smalley, J. Schmidt, Y. Talmon, Nano Lett. 3 (2003) 1379.
[37] M.S. Strano, C.B. Huffman, V.C. Moore, M.J. O'Connell, E.H. Haroz, J. Hubbard, M. Miller, K. Rialon, C. Kittrell, S. Ramesh, R.H. Hauge, R.E. Smalley, J. Phys. Chem. B 107 (2003) 6979.
[38] E.S. Jeng, J.D. Nelson, K.L.J. Prather, M.S. Strano, Small 6 (2010) 40.
[39] M.F. Islam, E. Rojas, D.M. Bergey, A.T. Johnson, A.G. Yodh, Nano Lett. 3 (2003) 269.
[40] Y.F. Ma, S.R. Ali, L. Wang, P.L. Chiu, R. Mendelsohn, H.X. He, J. Am. Chem. Soc. 128 (2006) 12064.
[41] M.S. Strano, M. Zheng, A. Jagota, G.B. Onoa, D.A. Heller, P.W. Barone, M.L. Usrey, Nano Lett. 4 (2004) 543.
[42] N.W.S. Kam, M. O'Connell, J.A. Wisdom, H.J. Dai, Proc. Natl. Acad. Sci. USA 102 (2005) 11600.
[43] N.W.S. Kam, Z. Liu, H.J. Dai, J. Am. Chem. Soc. 127 (2005) 12492.
[44] Z. Liu, X.M. Sun, N. Nakayama-Ratchford, H.J. Dai, ACS Nano 1 (2007) 50.
[45] J.H. Choi, M.S. Strano, Appl. Phys. Lett. 90 (2007) 22314.
[46] H. Jin, E.S. Jeng, D.A. Heller, P.V. Jena, R. Kirmse, J. Langowski, M.S. Strano, Macromolecules 40 (2007) 6731.
[47] P.W. Barone, H. Yoon, R. Ortiz-Garcia, J.Q. Zhang, J.H. Ahn, J.H. Kim, M.S. Strano, ACS Nano 3 (2009) 3869.
[48] C.A. Silvera-Batista, R.K. Wang, P. Weinberg, K.J. Ziegler, Phys. Chem. Chem. Phys. 12 (2010) 6990.
[49] R.K. Wang, W.C. Chen, D.K. Campos, K.J. Ziegler, J. Am. Chem. Soc. 130 (2008) 16330.
[50] P.W. Barone, S. Baik, D.A. Heller, M.S. Strano, Nat. Mater. 4 (2005) 86.
[51] D.A. Heller, E.S. Jeng, T.K. Yeung, B.M. Martinez, A.E. Moll, J.B. Gastala, M.S. Strano, Science (Washington, DC) 311 (2006) 508.
[52] P.W. Barone, M.S. Strano, Angew. Chem., Int. Ed. Engl. 45 (2006) 8138.
[53] E.S. Jeng, P.W. Barone, J.D. Nelson, M.S. Strano, Small 3 (2007) 1602.
[54] P.W. Barone, S. Baik, D.A. Heller, M.S. Strano, Electronic Properties of Novel Nanostructures, AIP Conf. Proc. 786 (2005) 193.
[55] V.A. Karachevtsev, A.Y. Glamazda, V.S. Leontiev, O.S. Lytvyn, U. Dettlaff-Weglikowska, Chem. Phys. Lett. 435 (2007) 104.
[56] C.H. Song, P.E. Pehrsson, W. Zhao, J. Mater. Res. 21 (2006) 2817.
[57] B.C. Satishkumar, L.O. Brown, Y. Gao, C.C. Wang, H.L. Wang, S.K. Doorn, Nat. Nanotechnol. 2 (2007) 560.
[58] H. Jin, D.A. Heller, M. Kalbacova, J.H. Kim, J.Q. Zhang, A.A. Boghossian, N. Maheshri, M.S. Strano, Nat. Nanotechnol. 5 (2010) 302.
[59] H. Jin, D.A. Heller, J.H. Kim, M.S. Strano, Nano Lett. 8 (2008) 4299.
[60] J.H. Kim, D.A. Heller, H. Jin, P.W. Barone, C. Song, J. Zhang, L.J. Trudel, G.N. Wogan, S.R. Tannenbaum, M.S. Strano, Nat. Chem. 1 (2009) 473.
[61] M.H. Lim, D. Xu, S.J. Lippard, Nat. Chem. Biol. 2 (2006) 375.
[62] J.H. Kim, J.H. Ahn, P.W. Barone, H. Jin, J.Q. Zhang, D.A. Heller, M.S. Strano, Angew. Chem., Int. Ed. Engl. 49 (2010) 1456.
[63] D.A. Heller, H. Jin, B.M. Martinez, D. Patel, B.M. Miller, T.K. Yeung, P.V. Jena, C. Hobartner, T. Ha, S.K. Silverman, M.S. Strano, Nat. Nanotechnol. 4 (2009) 114.
[64] P.W. Barone, R.S. Parker, M.S. Strano, Anal. Chem. 77 (2005) 7556.
[65] P. Cherukuri, C.J. Gannon, T.K. Leeuw, H.K. Schmidt, R.E. Smalley, S.A. Curley, R.B. Weisman, Proc. Natl. Acad. Sci. USA 103 (2006) 18882.
[66] K. Kostarelos, L. Lacerda, G. Pastorin, W. Wu, S. Wieckowski, J. Luangsivilay, S. Godefroy, D. Pantarotto, J.P. Briand, S. Muller, M. Prato, A. Bianco, Nat. Nanotechnol. 2 (2007) 108.
[67] T.K. Leeuw, R.M. Reith, R.A. Simonette, M.E. Harden, P. Cherukuri, D.A. Tsyboulski, K.M. Beckingham, R.B. Weisman, Nano Lett. 7 (2007) 2650.
[68] D. Pantarotto, R. Singh, D. McCarthy, M. Erhardt, J.P. Briand, M. Prato, K. Kostarelos, A. Bianco, Angew. Chem., Int. Ed. Engl. 43 (2004) 5242.
[69] R. Singh, D. Pantarotto, D. McCarthy, O. Chaloin, J. Hoebeke, C.D. Partidos, J.P. Briand, M. Prato, A. Bianco, K. Kostarelos, J. Am. Chem. Soc. 127 (2005) 4388.
[70] D. Pantarotto, J.P. Briand, M. Prato, A. Bianco, Chem. Commun. (2004) 16.
[71] J. Lefebvre, D.G. Austing, J. Bond, P. Finnie, Nano Lett. 6 (2006) 1603.
[72] D.A. Tsyboulski, S.M. Bachilo, R.B. Weisman, Nano Lett. 5 (2005) 975.
[73] H. Hong, T. Gao, W.B. Cai, Nano Today 4 (2009) 252.
[74] P. Cherukuri, S.M. Bachilo, S.H. Litovsky, R.B. Weisman, J. Am. Chem. Soc. 126 (2004) 15638.

[75] K. Welsher, Z. Liu, D. Daranciang, H. Dai, Nano Lett. 8 (2008) 586.
[76] H. Jin, D.A. Heller, R. Sharma, M.S. Strano, ACS Nano 3 (2009) 149.
[77] H. Jin, D.A. Heller, M.S. Strano, Nano Lett. 8 (2008) 1577.
[78] M.L. Becker, J.A. Fagan, N.D. Gallant, B.J. Bauer, V. Bajpai, E.K. Hobbie, S.H. Lacerda, K.B. Migler, J.P. Jakupciak, Adv. Mater. 19 (2007) 939.
[79] D.A. Heller, S. Baik, T.E. Eurell, M.S. Strano, Adv. Mater. 17 (2005) 2793.